AD-A129 546 PARAMETER SURVEY FOR COLLISIONLESS COUPLING IN A LASER SIMULATION OF HANE..(U) NAVAL RESEARCH LAB WASHINGTON DC R A SMITH ET AL. 01 JUN 83 NRL-MR-5092 1/1

UNCLASSIFIED F/G 18/3 NL

END
DATE
FILMED
7 83
DTIC

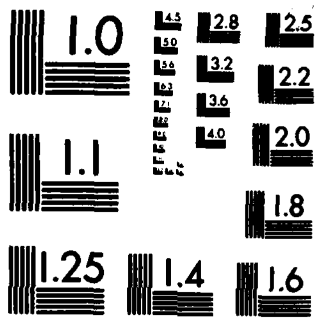

MICROCOPY RESOLUTION TEST CHART
NATIONAL BUREAU OF STANDARDS-1963-A

ADA129540

SECURITY CLASSIFICATION OF THIS PAGE (When Data Entered)

REPORT DOCUMENTATION PAGE		READ INSTRUCTIONS BEFORE COMPLETING FORM
1. REPORT NUMBER NRL Memorandum Report 5092	2. GOVT ACCESSION NO. AD-A129546	3. RECIPIENT'S CATALOG NUMBER
4. TITLE (and Subtitle) PARAMETER SURVEY FOR COLLISIONLESS COUPLING IN A LASER SIMULATION OF HANE		5. TYPE OF REPORT & PERIOD COVERED Interim report on a continuing NRL problem. 6. PERFORMING ORG. REPORT NUMBER
7. AUTHOR(s) R.A. Smith* and J.D. Huba		8. CONTRACT OR GRANT NUMBER(s)
9. PERFORMING ORGANIZATION NAME AND ADDRESS Naval Research Laboratory Washington, D.C. 20375		10. PROGRAM ELEMENT, PROJECT, TASK AREA & WORK UNIT NUMBERS 62715H; 47-0889-0-3
11. CONTROLLING OFFICE NAME AND ADDRESS Defense Nuclear Agency Washington, D.C. 20305		12. REPORT DATE June 1, 1983 13. NUMBER OF PAGES 36
14. MONITORING AGENCY NAME & ADDRESS (if different from Controlling Office)		15. SECURITY CLASS. (of this report) UNCLASSIFIED 15a. DECLASSIFICATION/DOWNGRADING SCHEDULE

16. DISTRIBUTION STATEMENT (of this Report)

Approved for public release; distribution unlimited.

17. DISTRIBUTION STATEMENT (of the abstract entered in Block 20, if different from Report)

18. SUPPLEMENTARY NOTES

*Present address: Science Applications, Inc., McLean, VA 22102.
This research was sponsored by the Defense Nuclear Agency under Subtask S99QMXBC, work unit 00067 and work unit title "Plasma Structure Evolution."

19. KEY WORDS (Continue on reverse side if necessary and identify by block number)

HANE coupling
Turbulent coupling
Laser simulation of HANE

20. ABSTRACT (Continue on reverse side if necessary and identify by block number)

We present a set of criteria for collisionless coupling of debris-air plasmas via the magnetized ion-ion instability (MII) for conditions relevant to the NRL DNA laser experiment. The criteria are based upon (1) a transit time of ions across the coupling shell sufficiently long to allow significant momentum exchange between the debris and air ions; (2) non-stabilization of the MII by electromagnetic effects; (3) a system size -> cont.

(Continues)

DD FORM 1 JAN 73 1473 EDITION OF 1 NOV 65 IS OBSOLETE
S/N 0102-014-6601

SECURITY CLASSIFICATION OF THIS PAGE (When Data Entered)

20. ABSTRACT (Continued)

cont

Beta

sufficiently large to contain at least a target mass of background gas; and (4) allowance for a high β expansion (i.e., super-Alfvenic expansion). A series of figures are presented which display these criteria graphically and indicate the coupling regime for parameters pertinent to the NRL experiment. We conclude that the proposed NRL upgraded facility (e.g., stronger magnetic field and larger target chamber) should be adequate to test the collisionless coupling criteria set forth in Lampe, et al. (1975).

CONTENTS

Accession For

NTIS GRA&I ☒
DTIC TAB ☐
Unannounced ☐
Justification

By
Distribution/

Availability Codes

Dist | Avail and/or Special
A

PARAMETER SURVEY FOR COLLISIONLESS COUPLING IN A LASER SIMULATION OF HANE

I. INTRODUCTION

It is well known that a high altitude nuclear explosion (HANE) can significantly disturb the natural ionosphere by producing large-scale, long-lasting ionization irregularities. These irregularities can have an adverse effect on radar and communication systems (e.g., scintillations). Thus, in order to understand and aid the operation of such systems in a nuclear environment, it is crucial to determine the behavior of the ionosphere following a HANE. To this end, DNA has supported an extensive research effort, both experimental and theoretical, to investigate the dynamics of the debris-air interaction and the subsequent evolution of the plasmas. The experimental research has involved laboratory experiments in the early 1970's (NRL, AVCO) and plasma cloud releases in the ionosphere; the theoretical research has been directed at developing advanced computer codes to model a HANE, and using naturally occurring and man-made ionospheric phenomena as a test bed for the HANE theories and codes.

Recently renewed interest in the laboratory simulation of a HANE has been stimulated in the DNA community (Vesecky et al., 1980; Cornwall et al., 1981). Longmire et al. (1981) have examined the scaling of a HANE to a laboratory experiment in which a target is "exploded" using a laser. One of the purposes of such an experiment would be to simulate the early-time phase of a HANE, and to determine whether or not collisionless coupling between the debris and air, via plasma microturbulence, is an important process. Longmire et al. (1981) concluded that such an experiment is feasible although non-trivial. Tsai et al. (1982) have re-examined the scaling laws involved between a HANE and a laser simulation. They have found that a "faithful" simulation of early-time phenomena is not possible in the laboratory as it would require extremely large magnetic fields ($B \sim$ few x 10^6 G) and densities ($n \sim$ solid state). However, they derive a set of "approximate" scaling laws which are amenable to laboratory conditions, and which should allow insight into the physics of the debris-air interaction. They conclude that the experimental facilities at NRL are adequate to perform such a simulation.

The purpose of this report is to examine the plasma conditions necessary (and hopefully achievable) for collisionless debris-air coupling to occur in the NRL experiment. The primary use of this work will be for

Manuscript approved March 28, 1983.

the experimentalists to use as a rough guide in choosing the appropriate parameters for the experiment (e.g., density, magnetic field, laser energy, targets and background gas). Thus, we present a series of graphs which indicate expected coupling regimes, based upon the magnetized ion-ion instability, as a function of laser energy, background gas density and atomic mass, and magnetic field strength. The important coupling physics issues used in this analysis are the following.

1. Magnetized ion-ion instability: We believe that the dominant instability that will lead to debris-air coupling is the magnetized ion-ion instability. The requirement for instability that may pose a problem in the simulation is $V_{da} < \alpha V_{Aa}$ where α is a parameter of order unity and is a function of the plasma conditions, V_{da} is the relative debris-air velocity in the radial direction and V_{Aa} is the Alfvén velocity.

2. System size: We require that the size of the experiment be greater than a mass radius, i.e., $L_s > R_w$ where L_s is the size of the experiment and R_w is the mass radius defined by $(4\pi/3)\rho_a R_w^3 = M_d$. Here, ρ_a is the background gas density and M_d is the debris mass.

3. Coupling time: We require that the instability occurs on a sufficiently fast time scale so that coupling can occur, i.e., $\nu_c \tau_{tr} > 1$ where ν_c is the effective collision frequency, $\tau_{tr} = \Delta/V_{da}$ is the transit time of an air ion in the debris, and Δ is the width of the coupling shell.

4. Magnetic field compression: We incorporate magnetic field compression in the criteria which depend upon the field. The relationship used is $B_c/B_0 = R/2\Delta$ where B_c is the compressed field, B_0 is the ambient field, R is the expansion radius of the debris shell, and Δ is the width of the debris shell (Wright, 1972).

The organization of the paper is as follows. In the next section, we discuss in greater detail the important physics issues upon which we base our analysis and which we believe are relevant to the NRL laser simulation. In Section III we discuss our results as they apply to the simulation and present figures indicating "coupling regimes." In the final section we discuss the implications of this work, as well as the limitations of the theory. Throughout the paper we use the expressions target and debris interchangeably, as well as background gas and air. We

conclude that there exist parameter regimes, which will be accessible to the NRL laser facility, in which collisionless coupling should occur.

II. COUPLING INSTABILITIES

In the mid-1970s, the NRL theory group studied a variety of plasma microinstabilities within the context of HANE (Lampe et al., 1975). The purpose of this research was to describe physical processes which could couple the debris-air plasmas, and provide a mechanism to heat the plasmas. The basic physical process involved is the "scattering" of particles from collective, fluctuating fields, associated with the instabilities, which can provide "anomalous transport coefficients" substantially larger than classical transport coefficients. We now give a brief overview of the instabilities considered by Lampe et al. (1975) which can lead to debris-air coupling and discuss their potential importance in regard to the laser simulation.

Prior to discussing the various instabilities, we first present Figs. 1 and 2 in order to indicate the geometry and the sources of free energy necessary to drive the plasma instabilities. In Fig. 1a we show the debris-air shell in the electron frame of reference. The debris is streaming in the radial (or x) direction; relative to the debris, the air plasma is streaming opposite to the debris (the -r or -x direction). Thus, in the radial (or x) direction there are <u>three</u> relative streaming velocities which can provide energy for an instability. They are (1) the relative debris-air velocity ($V_{da} = V_d - V_a$); (2) the relative debris-electron velocity ($V_{de} = V_d$); and (3) the relative air-electron velocity = ($V_{ae} = V_a$). There are also azimuthal currents (in the θ or y direction) which are set up to support the magnetic field gradients shown in Fig. 1b. These currents are driven by electron flow so that only a relative electron-ion drift exists in this direction $\left(\underset{\sim}{J} = -n_e V_e \hat{e}_{\theta,y}\right)$.

The slab geometry and plasma configuration appropriate to early-time is shown in Fig. 2. The ambient magnetic field and plasma parameters (density (n) and temperature (T)) are functions of r or x. The flows for the ions and electrons are, respectively,

$$\underset{\sim}{V}_i = (V_d - V_a)\hat{e}_{r,x} \tag{1}$$

and

$$\underset{\sim}{V}_e = V_e \hat{e}_{\theta,y} \qquad (2)$$

Strictly speaking, both $\underset{\sim}{V}_i$ and $\underset{\sim}{V}_e$ are also functions of x in the coupling shell; these inhomogeneities were ignored in Lampe et al. (1975) and will also be neglected in the present analysis. However, we note that such velocity inhomogeneities may affect the plasma instabilities under consideration. We defer such an analysis to a future report.

It is clear that two generic types of instabilities may exist in the early-time debris-air interaction: ion-ion streaming instabilities and electron-ion streaming instabilities. The ion-ion instabilities (i.e., magnetized ion-ion and unmagnetized ion-ion) occur only in the radial (or x) direction and can provide momentum transfer between the debris and air (i.e., coupling) and can heat the ions (Papadopoulos et al., 1971). The electron-ion instabilities (i.e., modified two stream, beam cyclotron, ion acoustic) can occur in both the radial (or x) and azimuthal (or y) directions. These instabilities primarily heat electrons, although the radial modified two stream instability can provide debris-air coupling (McBride et al., 1972). The azimuthal electron-ion instabilities limit the size of the magnetic field gradients and can cause radial diffusion of the magnetic field, density and temperature. Since the main emphasis of the laser simulation is on debris-air coupling, we restrict our attention to those instabilities which occur in the radial (or x) direction and can provide debris-air coupling: the unmagnetized and magnetized ion-ion instabilities, and the modified two stream instability.

A. Unmagnetized ion-ion instability

The turn-on conditions for the unmagnetized ion-ion instability (UII) is given by (Lampe et al., 1975)

$$\frac{V_{ji}}{v_j} \gtrsim 4\ \alpha_{ji}^{-1/3} \qquad (3)$$

and

$$\frac{V_{ji}}{v_i} \gtrsim 2 \qquad (4)$$

where

$$\alpha_{ji} = \frac{n_j Z_j^2 m_i}{n_i Z_i^2 m_j} \lesssim 1, \tag{5}$$

$V_{ji} = |\underset{\sim}{V}_{ji}| = |\underset{\sim}{V}_j - \underset{\sim}{V}_i|$ is the relative streaming velocity between the ion species (i.e., debris and air), v is the thermal velocity, n is the density, Z is the charge, and m is the mass of each species accordingly. In the laser simulations to date, it appears that that these conditions are easily satisfied since $V_{da}/v_d \sim 8$ and $V_{da}/v_a \sim 10$ (B. Ripin, private communication).

However, in order to prevent the instability from being stabilized by electron shielding it is necessary that

$$V_{ji} < 1.5\, c_i (1 + \alpha_{ji}^{1/3})^{3/2} \tag{6}$$

where

$$c_i = \left(\frac{n_i Z_i^2 T_e}{n_e m_i}\right)^{1/2}. \tag{7}$$

Assuming a = i, d = j, $n_a/n_e \sim 1/2$, $\alpha_{da} \sim 1/2$, and $V_{da} \sim 6 \times 10^7$cm/sec, we find that

$$T_e > 550 \frac{A_a}{Z_a} \text{ eV} \tag{7}$$

where A_a and Z_a are the atomic mass and charge state of the background gas. It is believed that the electron temperature in the laser simulation is $T_e \sim 100$ eV in the debris shell shortly after the laser pulse has been terminated (B. Ripin, private communication), so that it is unlikely that the unmagnetized ion-ion instability will occur (this is especially true for an air background).

B. Magnetized ion-ion instablity

The turn-on conditions for the magnetized ion-ion instability (MII) are the same as in the case of the unmagnetized ion-ion instability (Eqs. (3) and (4)) and these criteria should be satisfied in the laser experiment. On the other hand, in order to avoid electromagnetic stabilization of the instability, it is required that

$$V_{ji} < \alpha_0 V_{Ai} \tag{9}$$

where $\alpha_0 \sim O(1)$ and is

$$\alpha_0 = 1.2\left(\frac{n_i}{n_e}\right) Z_i \left(1 + \alpha_{ji}^{1/3}\right)^{3/2} \left(1 + \beta_e\right)^{1/2}. \tag{10}$$

Here, $\beta_e = 8\pi n_e T_e / B^2$ and $V_{Ai} = B/(4\pi n_i m_i)^{1/2}$.

Another criterion for instability discussed in Lampe et al. (1975) is

$$L_s > \alpha_1 \frac{V_{di}}{\Omega_p} \tag{11}$$

where L_s is the system size and $\alpha_1 \sim O(1)$ and is

$$\alpha_1 = 4.4\left(\frac{n_e^2 A_i A_j}{n_i n_j Z_i Z_j}\right)^{1/2} \left(1 + \alpha_{ji}^{1/3}\right)^{3/2} \tag{12}$$

Also, $\Omega_p = e\,B/m_p c$ and m_p is the proton mass. Equation (11) is a statement that the parallel wavelength associated with the instability is small enough to fit into the system. As a rough estimate of L_s for the simulation, we assume $V_{da} \sim 6 \times 10^7$ cm/sec and $B \sim 2 \times 10^3$ so that $L_s > 3$ cm is required. We note that this system size will be achievable in the NRL experiment. We also comment that Eq. (11) may not be required since the magnetized ion-ion instability is insensitive to the particle dynamics parallel to the field. A careful treatment of the influence of parallel wave effects on the instability in a magnetic field profile appropriate to a HANE and the experiment is needed. Thus, we do not consider this criterion as a major obstacle to the experiment.

C. Modified two stream instability

The turn-on condition for the modified two stream is

$$V_{ie} > 2v_i \tag{13}$$

where $V_{ie} = V_d$ or V_a, depending upon which ion species is being considered and v_i is the corresponding thermal velocity of the ions. This condition is likely to be met in the NRL simulation. In order to avoid electromagnetic stabilization of this instability, it is required that

$$V_{ie} < \alpha_2 V_{Ai} \tag{14}$$

where $\alpha_2 \sim O(1)$ and is

$$\alpha_2 = \frac{n_i}{n_e} Z_i (1 + \beta_e)^{1/2} g \tag{15}$$

where g is a function of order unity (Lampe et al., 1975 - see p. 10 and 11).

Finally, there is also a condition on the size of the system given roughly by

$$L_s > 2\pi\alpha_3 \frac{V_{ie}}{\omega_{Hi}} \left(\frac{m_i}{m_e}\right)^{1/2} \tag{16}$$

where $\alpha_3 = 1/\Theta(1 + \Theta)$, $\Theta \sim O(1)$ and $\omega_{Hi} = \omega_{pi}/(1 + \omega_{pe}^2/\Omega_e^2)^{1/2}$. We note that Eq. (16) is an important consideration for the modified two stream instability since the instability relies upon the electron dynamics parallel to the magnetic field. Assuming $V_{ie} \sim 3 \times 10^7$ cm/sec and $B \sim 2 \times 10^3$ G, we find $L_s > 6$ cm which is somewhat more restrictive than the magnetized ion-ion condition.

Based upon the criteria outlined for the various ion-ion coupling instabilities, and the expected operating conditions of the NRL laser experiment, we believe the most likely and the most important coupling instability to be excited is the magnetized ion-ion instability. The unmagnetized ion-ion instability will only be excited if the electrons can be heated to high temperatures ($T_e \gtrsim 1$ keV) which is not expected to occur

in the experiment after the laser beam is terminated. The modified two stream instability is more restricted by the system size is than the magnetized ion-ion instability. The modified two stream instability may be excited in the experiment, but the coupling criteria are similar to those of the magnetized ion-ion instability. Thus, in estimating the appropriate parameters to be used in laser experiment, we base our analysis on the criteria associated with the magnetized ion-ion instability. Aside from the turn-on conditions associated with the MII instability, the remaining crucial parameter to be stated is the effective collision frequency (or anomalous collsion frequency) produced by the this instability. This collision frequency is (Lampe et al., 1975)

$$\nu_{ij} = 0.15\ \omega_{Hi} \frac{\rho_i}{\rho} f(\alpha_{ji}) \tag{17}$$

where $\omega_{Hi} = \omega_{pi}/(1 + \omega_{pe}^2/\Omega_e^2)^{1/2}$, ρ is the mass density, and

$$f(\alpha_{ji}) = \alpha_{ji}^{2/3} + (3^{1/2}/2^{1/3})\ (\alpha_{ji}^{1/3} - \alpha_{ji}^{2/3}). \tag{18}$$

III. COUPLING CRITERIA

The theory of the various instabilities of interest, even in the simplified local form presented by Lampe et al. (1975), involves many parameters that vary in a complicated manner, both in time and space, during the early-time expansion. Thus, detailed theoretical predictions of the coupling are difficult, and so our approach is to attempt to relate the local description of the instability condition of Lampe et al. (1975), through some simplifying heuristic criteria, to initial conditions and parameters which are controllable in the experiment. Examples of such parameters are the ambient magnetic field strength B_0, the expansion velocity V_d, the ambient background density n_a, the kinetic yield of the target W, and so forth. We may then hope to provide, as initial guidance for the experiment design, parameter envelopes within which short-scale-length coupling might be expected to occur.

We stress that such estimates are approximate. Moreover, we have not yet attempted to relate the resulting parameter spaces to the scaling criteria developed by other authors, e.g., Longmire et al. (1981) or Tsai et al. (1982), for several reasons. First, we expect that the experimental phenomenology will still be of interest to HANE so long as qualitative scaling is preserved, i.e., most dimensionless ratios which are small, of order unity, or large in HANE are, respectively, small, of order unity, or large in the experiment, without necessarily translating the exact scaling (Tsai et al., 1982). Second, it may be desirable or even necessary to suppress certain effects in the experiment in order to provide an unambiguous test of short-scale-length coupling theory by isolating the parameter regime in which it is expected to dominate. For example, collisions and charge exchange can only provide complicating effects which may mask the conclusions regarding short-scale-length coupling, especially insofar as some of the chemical reactions which may enter at higher density (such as ternary reactions) do not scale correctly.

A. Defi ition of the coupling criteria

The basic criteria we adopt are the following:

1. Transit-time criterion

We require that a parcel of air (or background gas) spend at least one momentum-transfer time constant in traversing the coupling shell. The coupling shell thickness is denoted by $\Delta(R)$ at some expansion radius R and has a nominal expansion velocity $V_d(R)$ through a stationary background gas (i.e., $V_a = 0$). Denoting the anomalous collision frequency for momentum transfer from the debris to the ambient gas by ν_{ad}, we then have

$$\nu_{ad}\tau_{tr} = \frac{\nu_{ad}\Delta}{V_d} > 1. \qquad (19)$$

We adopt (19) as a physically reasonable estimate since the wave turbulence to produce coupling primarily occurs in the coupling shell. Also, we evaluate Eq. (19) at $R = R_w$ since collisionless coupling is strongest at roughly R_w (R. Clark, private communication).

2. Non-stabilization by electromagnetic effects

The magnetized ion-ion instability is stabilized by electromagnetic effects unless Eq. (9) is satisfied.

3. System-size criterion

Assuming that coupling occurs near the radius at a target mass R_w, we require

$$R_w \ll L, \tag{20}$$

where L is the characteristic system dimension, i.e., the size of the laser target chamber.

4. High-beta expansion criterion

In order that the debris not expend a major fraction of its energy in field compression (which may then be mistaken for short-scale-length coupling) we require

$$R_w \ll R_B \tag{21}$$

where R_B is the radius of a volume containing magnetic energy equal to the kinetic yield:

$$R_B = \left(\frac{6W}{B_0^2}\right)^{1/3} \tag{22}$$

Note that because of the R^3 dependence of a spherical expansion, inequality (22) is already strong for $R_w \lesssim R_B/2$.

B. Quantitative evaluation of the criteria

The intial parameters that may be easily controlled experimentally, i.e., those which may be varied over the widest range, are the ambient background gas density n_a and the kinetic yield W. We shall cast the coupling criteria outlined above into inequalities relating these two quantities. Eventually, the experimentalists will have control over the ambient magnetic field and we will also present results with this quantity as a control variable.

In order to evaluate the coupling criteria, several quantities need to be calculated: (1) $\Delta(R_w)$ - the coupling shell width at a mass radius; (2) n_d/n_a - the ratio of the debris density to the background gas density; and (3) B_c/B_0 - the ratio of the compressed magnetic field to the ambient magnetic field. We now discuss each of these quantities.

We approximate the shell thickness Δ by

$$\Delta(R) \simeq V_d \tau_\ell + \frac{\Delta V_d}{V_d} R \tag{22}$$

where τ_ℓ is the length of the laser pulse, ΔV_d is the thermal spread in the velocity of the debris, V_d is the expansion velocity, and R is the position of the coupling shell. Taking typical values for the NRL experiment, we assume $\tau_\ell \sim 4 \times 10^{-9}$ sec, $\eta_d \equiv \Delta V_d/V_d \sim .25$, $V_d \sim 4 \times 10^7$ cm/sec (B. Ripin, private communication), and $R = R_w$ so that

$$\Delta(R_w) \simeq .16 + .25\, R_w \text{ cm.} \tag{23}$$

Again, for typical experimental conditions we note that

$$R_w >> V_d \tau_\ell / \eta_d, \tag{24}$$

so Eq. (23) becomes

$$\Delta(R_w) \simeq \eta_d R_w \simeq R_w/4. \tag{25}$$

The ratio of the debris density to the background gas density is a function of position in the coupling shell. Rather than consider a variety of values, we use the average debris density in the coupling shell. This is a simplifying assumption and our results are not overly sensitive to this parameter. The average debris density in the coupling shell is given by

$$\bar{n}_d \sim \frac{M_d}{4\pi R_w^2 m_d \Delta} \sim \frac{M_d}{4\pi \eta_d R_w^3 m_d} \tag{26}$$

where M_d is the target mass and m_d is the mass of a debris ion. Making use of the defintion of R_w (i.e., $(4\pi/3)\rho_a R_w^3 = M_d$) we find that

$$\frac{\bar{n}_d}{n_a} \simeq \frac{A_a}{3\eta_d A_d} \tag{27}$$

Based on Eq. (27), we note that

$$\alpha_{da} \simeq \frac{Z_d^2}{Z_a^2} \frac{A_a^2}{A_d^2} \frac{1}{3\eta_d} \tag{28}$$

where $m_{a,d} = A_{a,d}\, m_p$ and m_p is the proton mass. Similarly, α_{ad} is defined

$$\alpha_{ad} = 3\eta_d \frac{Z_a^2 A_d^2}{Z_d^2 A_a^2}$$

Finally, we also need an estimate of the magnetic field compression in the coupling shell. A simple estimate based on the conservation of flux, as in the Longmire coupling shell model, gives the compressed field B_c (in the equatorial plane of the expansion) in terms of the ambient field B_0 as

$$\frac{B_c}{B_0} \sim \frac{R_w}{2\Delta} \sim \frac{1}{2\eta_d}. \tag{29}$$

We note that for $\eta_d \lesssim 1/4$ the field compression in the NRL experiment is expected to be modest, i.e., $B_c/B_0 \sim 2$, which is consistent with experimental results thus far (S. Kacenjar, private communication).

Based on the coupling criteria outlined in Section III.A and the quantities defined above, we now present a set of quantitative conditions required for collisionless coupling via the magnetized ion-ion instability in the NRL DNA laser experiment. We first define the following quantities to be used in our results:

$$f(\alpha_{ji}) = \alpha_{ji}^{2/3} + (3^{1/2}/2^{1/3})\,(\alpha_{ji}^{1/3} - \alpha_{ji}^{2/3}) \tag{30}$$

$$K_{ji} = f^{-1}(\alpha_{ji})\,[1 + \frac{n_j A_j}{n_i A_i}]\,(A_i/Z_i)^{1/2}\,[1 + \frac{n_j Z_j}{n_i Z_i}]^{1/2} \tag{31}$$

$$H_{da} = \frac{1}{\eta_d^2 A_a}\,[1 + \frac{A_a Z_d}{3\eta_d A_d Z_a}]^{-2}\,[1 + (\frac{1}{3\eta_d} \frac{A_a^2 Z_d^2}{A_d^2 Z_a^2})^{1/3}]^3 \tag{32}$$

$$H_{ad} = \frac{3}{\eta_d A_a}\,[1 + 3\eta_d \frac{Z_a A_d}{Z_d A_a}]^{-2}\,[1 + (3\eta_d \frac{A_d^2 Z_a^2}{A_a^2 Z_d^2})^{1/3}]^3 \tag{33}$$

$$V_{d7} = V_d/10^7 \text{ cm/sec} \tag{34}$$

$$B_{03} = B_0/10^3 \text{ G} \tag{35}$$

$$n_{a14} = n_a/10^{14} \text{ cm}^{-3} \tag{36}$$

Equations (34) - (36) are the debris velocity, ambient magnetic field, and background gas density, respectively, normalized to numerical values relevant to the experiment.

The coupling criteria are as follows.

1. Transit time criterion (τ_{tr})

$$W \geq 1.17 \times 10^{-4} A_a V_{d7}^5 \frac{n_{a14}}{B_{03}^3} \begin{cases} K_{da}^3 & ; \quad \alpha_{da} < 1 \\ K_{ad}^3 & ; \quad \alpha_{ad} < 1 \end{cases} \tag{37}$$

where W is the kinetic yield of the debris measured in joules.

2. Non-stabilization by electromagnetic effects (em)

$$n_{a14} \leq 1.50 \frac{B_{03}^2}{V_{d7}^2} \begin{cases} H_{da} & ; \quad \alpha_{da} < 1 \\ H_{ad} & ; \quad \alpha_{ad} < 1 \end{cases} \tag{38}$$

3. System size criterion (L)

$$W \leq 0.90 A_a V_{d7}^2 n_{a14} L^3 \tag{39}$$

Note that Eqs. (37) and (39) combine to give a minimum system length

$$L \geq 0.71 \frac{K_{ji}}{(A_a n_{a14})^{1/2}} \quad ; \quad \alpha_{ji} < 1 \tag{40}$$

4. High beta expansion (β)

$$n_{a14} \geq 4.80 \frac{B_{03}^2}{A_a V_{d7}^2} \tag{41}$$

C. Graphical presentation of coupling criteria

We now present a series of figures for various experimental parameters, such as target materials, background gases, debris velocities, and system sizes, as a function of kinetic yield, background gas density, and ambient magnetic field. These figures should serve as a guide to the experimentalists and be useful in designing experiments to test collisionless coupling of the debris-air plasmas via the magnetized ion-ion instability.

Schematically, the figures presented will correspond to those shown in Fig. 3 and are obtained as follows. First, the quantities A_a, A_d, Z_a, and Z_d are fixed at some specified values. A_a and A_d are the atomic masses (in proton units) of the background gas and the target material, respectively, and are known for each run. Z_a and Z_d are the charge states of the background and target plasmas, respectively, and are not well-known. We anticipate that many charge states will coexist and vary in time within the coupling shell. For the purpose of obtaining approximate coupling regimes we make the simplifying assumption of an average charge state for each ion species. The values chosen are based upon previous theoretical work (R. Clark, private communication) and experimental work (J. Grun, private communication). Second, the parameters B_0 and V_d (Fig. 3a) or n_a and V_d (Fig. 3b) are fixed at some relevant values, and conditions (37) - (41) are plotted as functions of kinetic yield W (in joules) versus the density n_a (Fig. 3a) or the ambient magnetic field B_0 (Fig. 3b). The boundary lines for each condition are denoted by τ_{tr} [Eq. (37)], em [Eq. (38)], L [Eq. (40)], and β [Eq. (41)], and are based upon solving these conditions as equalities. The shading indicates the side of the line for which the inequalities hold and indicate the parameters (W and n_a or W and B_0) needed for coupling. In both Figs. 3a and 3b, it is found that there is a coupling regime defined by a "box" or "window" in the parameter space (W, n_a) or (W, B_0). Figures 4 - 7 show some examples for parameters accessible (or eventually accessible) to the NRL laser facility.

Figures 4 and 5 are for an aluminum target (A_d = 29) with an average charge state of 10 (Z_d = 10), and a nitrogen background gas (A_a = 14) with an average charge state of 3 (Z_a = 3). Figure 4 displays kinetic yield W versus background density n_a for two sets of debris velocity and ambient

magnetic field values: (a) $V_d = 2 \times 10^7$ cm/sec and $B_0 = 800$ G and (b) $V_d = 4 \times 10^7$ cm/sec and $B_0 = 4000$ G. The first set of parameters is achievable with the present NRL laser facility. For this set, very low densities are required for coupling, 6×10^{12} cm^{-3} < n_a < 4×10^{13} cm^{-3}, and a larger system size (L > 5 cm) than is presently available (L ~ 3 cm). The second set of parameters uses a significantly larger ambient magnetic field $B_0 = 4000$ G (which should be obtainable in the experiment in the near future). It is found that coupling can occur for higher density plasmas 5×10^{13} cm^{-3} < n_a < 4×10^{14} cm^{-3} and smaller system sizes (L > 2 cm) than the previous case. Figure 5 is a plot a kinetic yield W versus the ambient magnetic field B_0. The species and charge states are the same as in Fig. 4 but a higher debris velocity is used ($V_d = 6 \times 10^7$ cm/sec) and the system size is taken, for illustration, to be 10 cm. The coupling regimes are shown for three sets of densities: $n_a = 10^{14}$, 10^{15}, and 10^{16} cm^{-3}. We note that as the density increases, the range of W and the magnitude of the ambient magnetic field required for coupling both increase. Since the ambient magnetic field in the NRL experiment will be such that $B_0 < 10$ kG, the experiment will require low density background plasmas ($n_a < 10^{15}$ cm^{-3}) to obtain coupling for an Al-N system. Thus, from Figs. 4 and 5 we find that the NRL DNA laser experiment should be able to achieve collisionless coupling via the MII instability using an aluminum target and a nitrogen background gas in future experiments using an upgraded magnetic field and target chamber. The present facility ($B_0 = 800$ G and L < 3 cm) is inadequate to obtain coupling based upon our criteria.

In Figs. 6 and 7 we present the coupling regimes analogous to Figs. 4 and 5 but using a carbon target ($A_d = 12$) with an average charge state of 4 ($Z_d = 4$) and a hydrogen background ($A_a = 1$) with a charge state of 1 ($Z_a = 1$). In Fig. 6 we plot W versus n_a for $V_d = 3 \times 10^7$ cm/sec, and $B_0 = 800$ G and 4000 G. It should be noted that for $B_0 = 800$ G, the required densities 3.5×10^{13} cm^{-3} < n_a < 2.8×10^{14} cm^{-3} are somewhat higher than those of the Al-N system (Fig. 4). However, larger kinetic yields are also required so that the coupling regime is somewhat smaller the Al-N system. Also, a large system size (L > 5.5 cm) is needed, greater than what is presently available. On the other hand, for $B_0 = 4000$ G, the densities required are in the range 8×10^{14} cm^{-3} < n_a < 6×10^{15} cm^{-3}, and the system size is L > 1.1 cm. In Fig. 7 we show W versus B_0 for $V_d = 6 \times 10^7$ cm/sec and L = 10

cm for three values of density: $n_a = 10^{14}$, 10^{15}, and 10^{16} cm^{-3}. The qualitative behavior of these curves are similar to Fig. 5. However, the quantitative behavior is more favorable to coupling in the upgraded NRL laser facility in that a larger range of densities is accessible for coupling in the regime $B_0 < 10$ kG, i.e., $n_a < 10^{16}$ cm^{-3} rather than $n_a < 10^{15}$ cm^{-3} for the Al-N system (Fig. 5).

IV. DISCUSSION

We have presented a set of criteria for collisionless coupling of debris-air plasmas via the magnetized ion-ion instability (Lampe et al., 1975) for conditions relevant to the NRL DNA laser experiment. The criteria are defined by Eqs. (37) - (41) and are based upon (1) a transit time of ions across the coupling shell sufficiently long to allow significant momentum exchange between the debris and air ions; (2) non-stabilization of the MII because of electromagnetic effects; (3) a system size (i.e., target chamber) sufficiently large to contain at least a target mass of background gas; and (4) allowance for a high β expansion, i.e., super-Alfvénic expansion. A series of figures (Figs. 4 -7) are presented which display these criteria graphically and which indicate coupling regimes for parameters pertinent to the NRL experiment. We have specifically considered experiments using both an aluminum target with a nitrogen background, and a carbon target with a hydrogen background. In gerneral, lighter target and background gases provide a broader (more easily accessible) range of experimental parameters for which collisionless coupling can occur. We conclude that the present NRL laser facility (B_0 = 800 G and $L < 4$ cm) is inadequate to allow collisionless coupling to occur, but that the proposed, upgraded facility ($B_0 < 10$ kG and $L < 10$ cm) is adequate to test the collisionless coupling criteria set forth in this analysis (Lampe et al., 1975).

Finally, we emphasize that this report has considered an idealized situation: several simplifying assumptions have been made in the analysis. First, we consider constant, average charge states of each ion species although it is clear that multiple charge states may exist that vary in time in the experiment (J. Grun, private communication). Second,

we consider fully ionized plasmas and ignore any collisional effects. Again, this assumption is an over-simplification and collisional effects need to be carefully addressed for interpretation of experimental results. For example, the pre-ionization of the background gas due to the initial radiation "flash" appears to be small (< a few percent at a mass radius) (Hyman et al., 1983), so that the expanding debris shell may collisionally ionize the background gas. And finally, we note that the chemistry and radiation physics associated with the experiment is critically dependent upon the types of targets and background gases used. It may be worthwhile in running experiments to use materials which have relatively simple chemistry and radiation physics (e.g., use a helium background gas instead of hydrogen). Nonetheless, we believe our results are a useful guide to the experimentalists as a first step in designing experiments to study collisionless coupling.

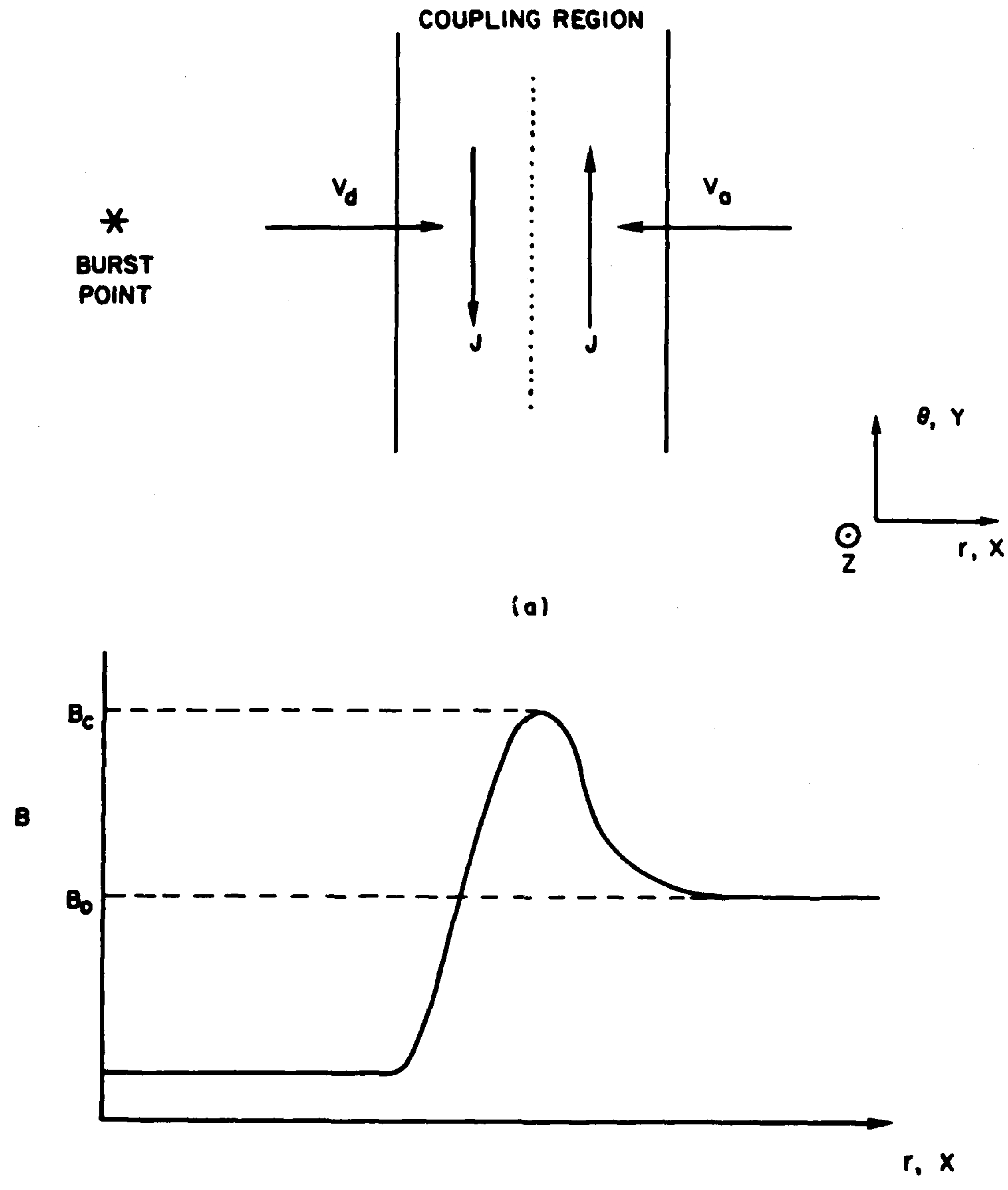

Figure 1

Schematic of relative drift velocities and magnetic field strength in the coupling shell following a HANE.

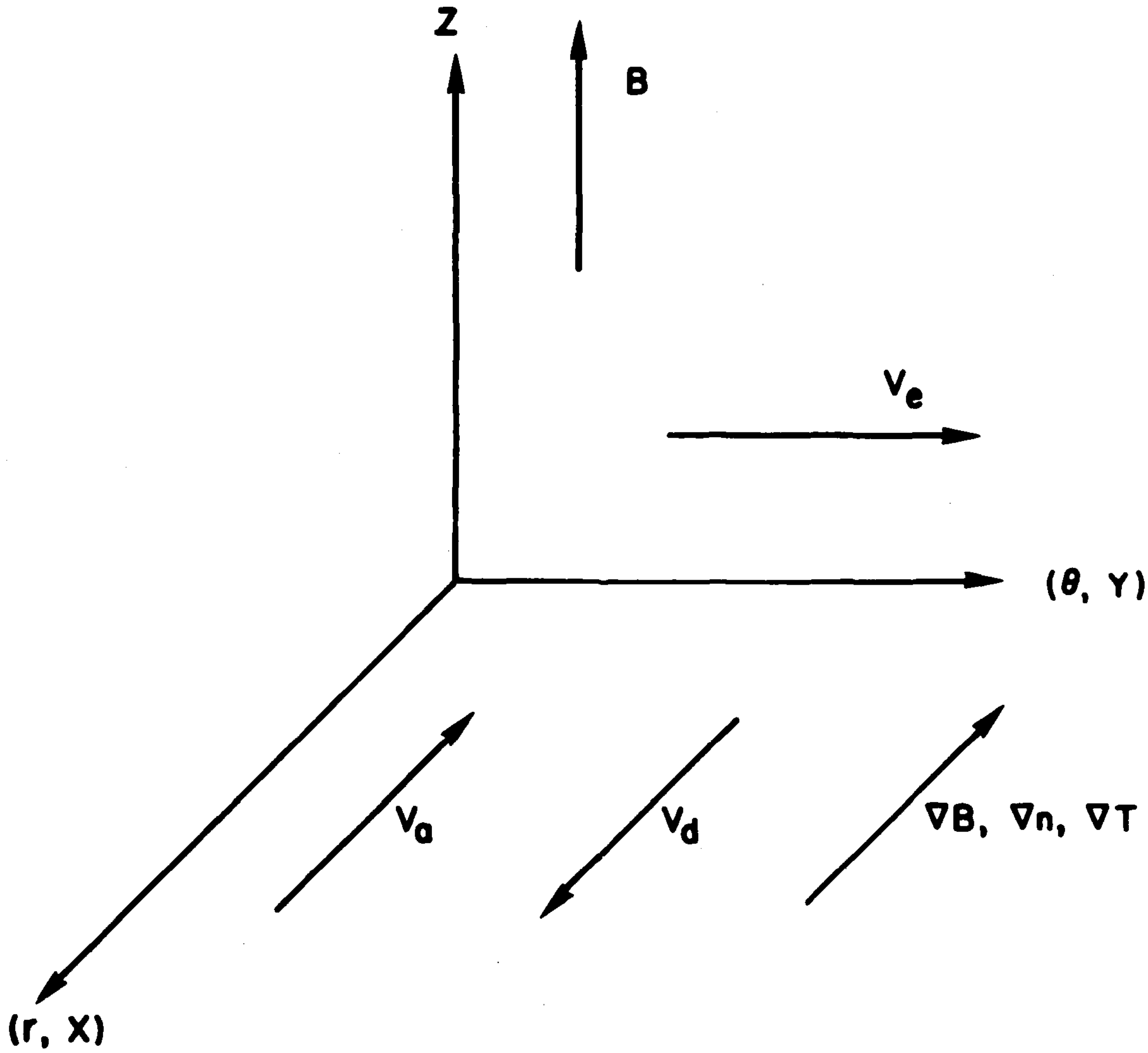

Figure 2

Slab geometry of the coupling shell region.

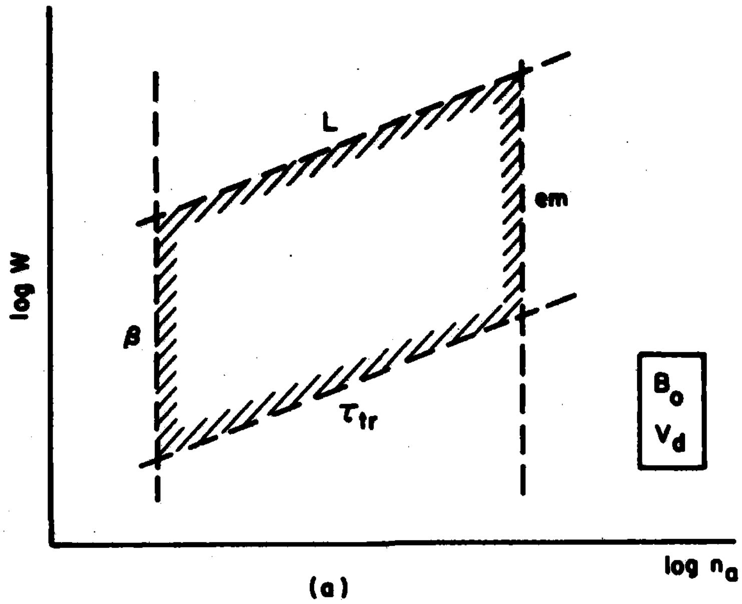

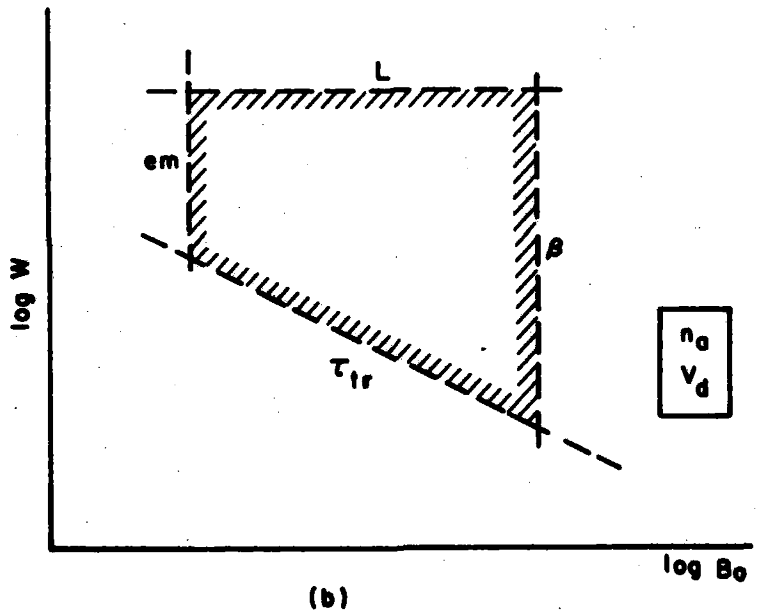

Figure 3

Schematic of coupling regime figures. The interior of the trapezoids (shaded side) indicate the parameters necessary for collisionless coupling. Here, τ_{tr}, em, L, and β denote the criteria defined by Eqs. (37) - (40), respectively. (a) Schematic of kinetic yield W versus background density n_a; B_0 and V_d must be specified. (b) Schematic of kinetic yield W versus ambient magnetic field B_0; n_a and V_d must be specified. In both (a) and (b), A_a, A_d, Z_a, and Z_d must be specified.

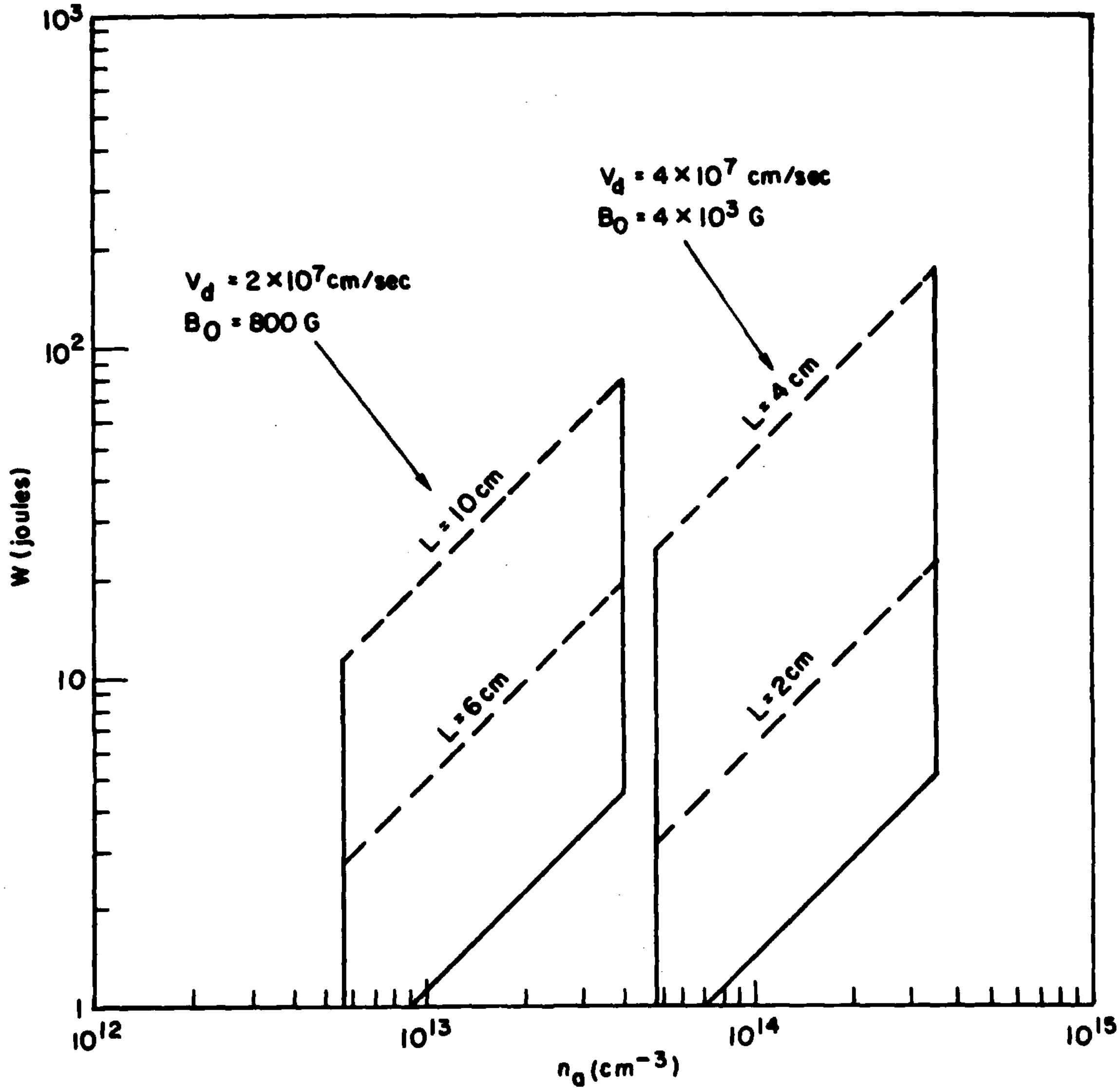

Figure 4

Plot of kinetic yield W (joules) versus background density n_a (cm^{-3}) for an aluminum target ($A_d = 29$) with an average charge state of 10 ($Z_d = 10$), and a nitrogen background gas ($A_a = 14$) with an average charge state of 3 ($Z_a = 3$). Two cases are considered: (1) $V_d = 2 \times 10^7$ cm/sec and $B_0 = 800$ G with L = 6 and 10 cm, and (2) $V_d = 4 \times 10^7$ cm/sec and $B_0 = 4000$ G with L = 2 and 4 cm.

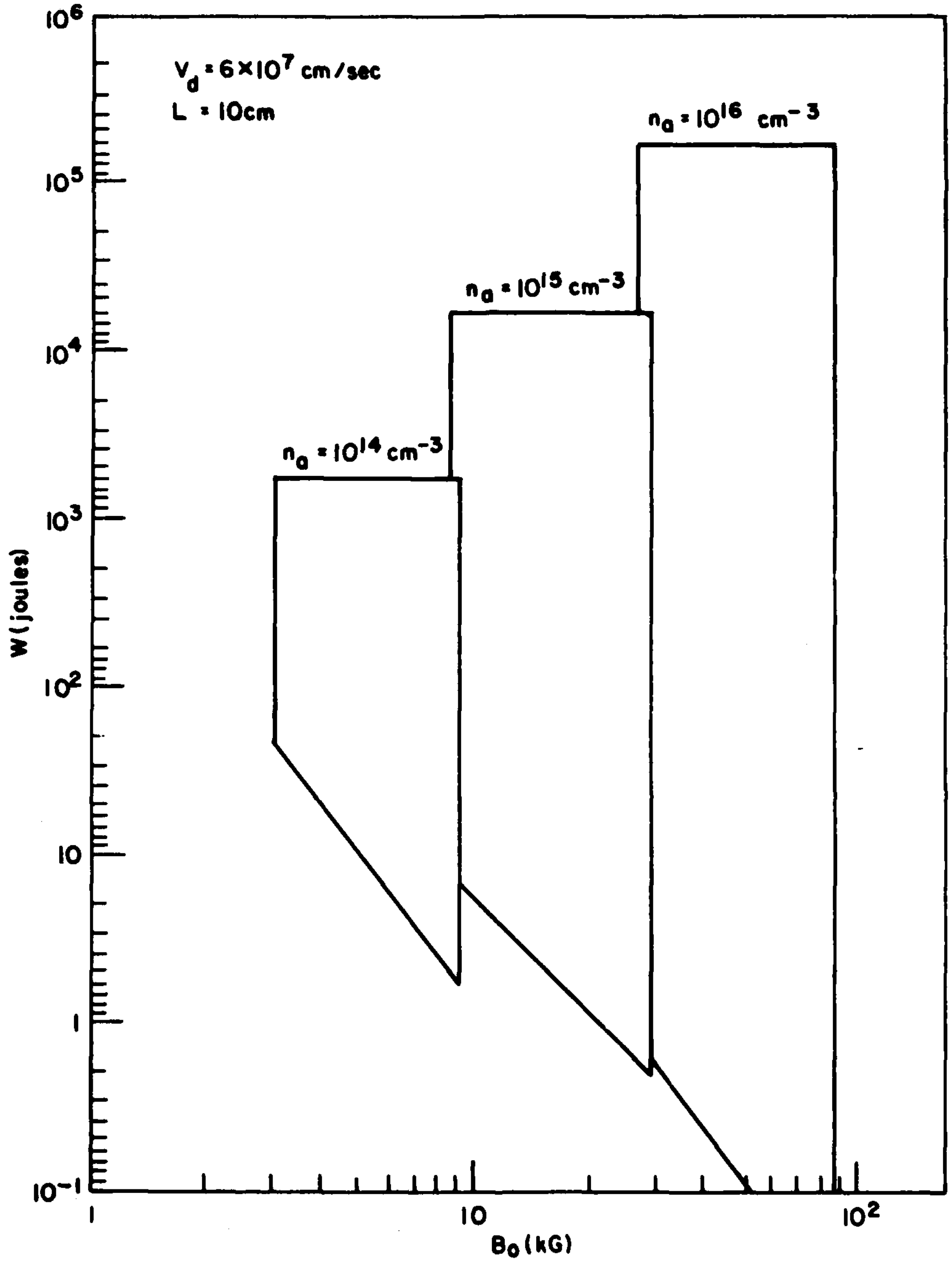

Figure 5

Plot of kinetic yield W (joules) versus ambient magnetic field B_0 (G) for the same target/gas as Fig. 4. We take $V_d = 6 \times 10^7$ cm/sec, L = 10 cm, and $n_a = 10^{14}$, 10^{15}, and 10^{16} cm^{-3}.

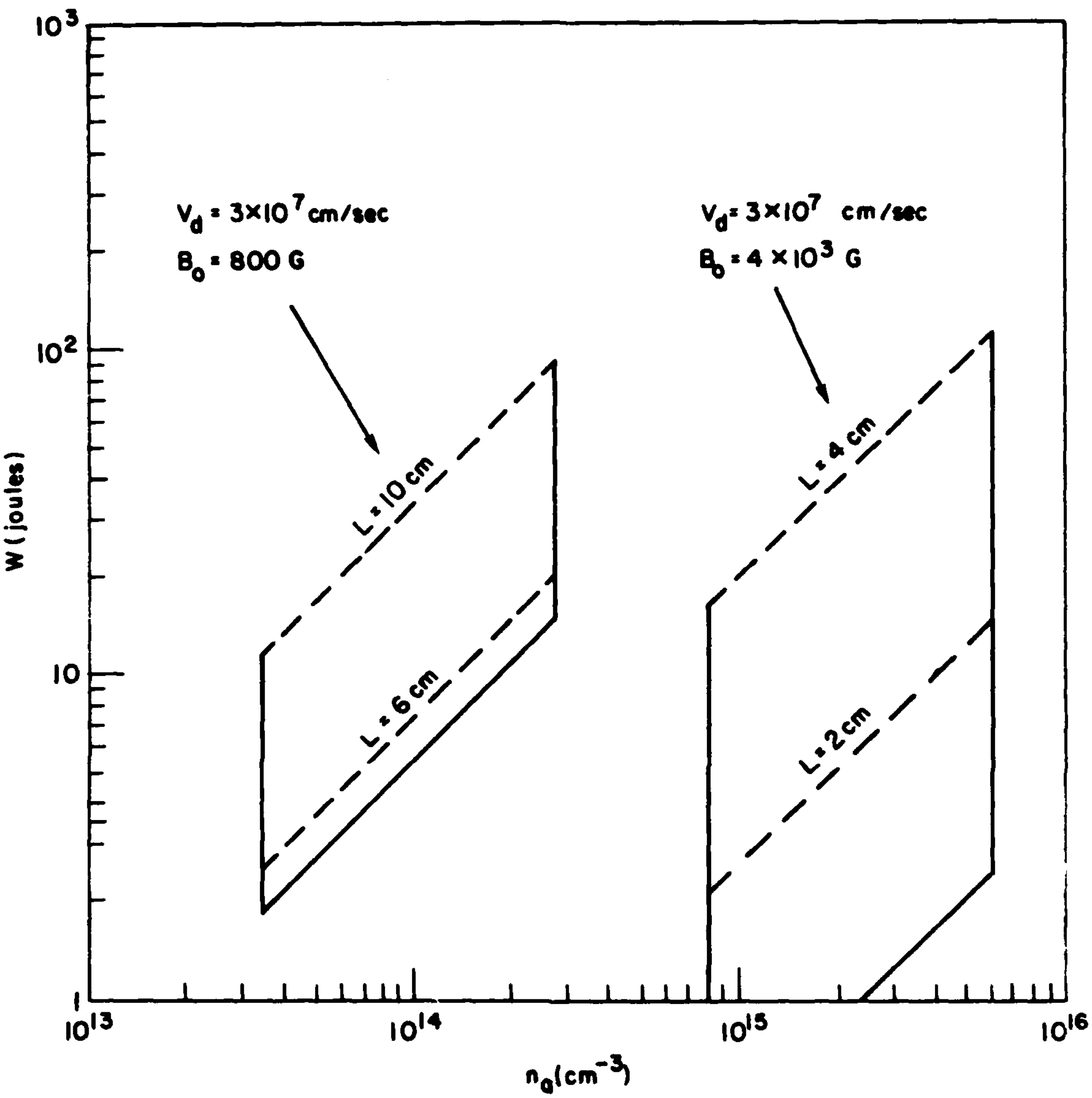

Figure 6

Plot of kinetic yield W (joules) versus background density n_a (cm^{-3}) for a carbon target (A_d = 12) with an average charge state of 4 (Z_d = 4), and a hydrogen background gas (A_a = 1) with a charge state of 1 (Z_a = 1). Two cases are considered: (1) $V_d = 3 \times 10^7$ cm/sec and B_0 = 800 G with L = 6 and 10 cm, and (2) $V_d = 3 \times 10^7$ cm/sec and B_0 = 4000 G with L = 2 and 4 cm.

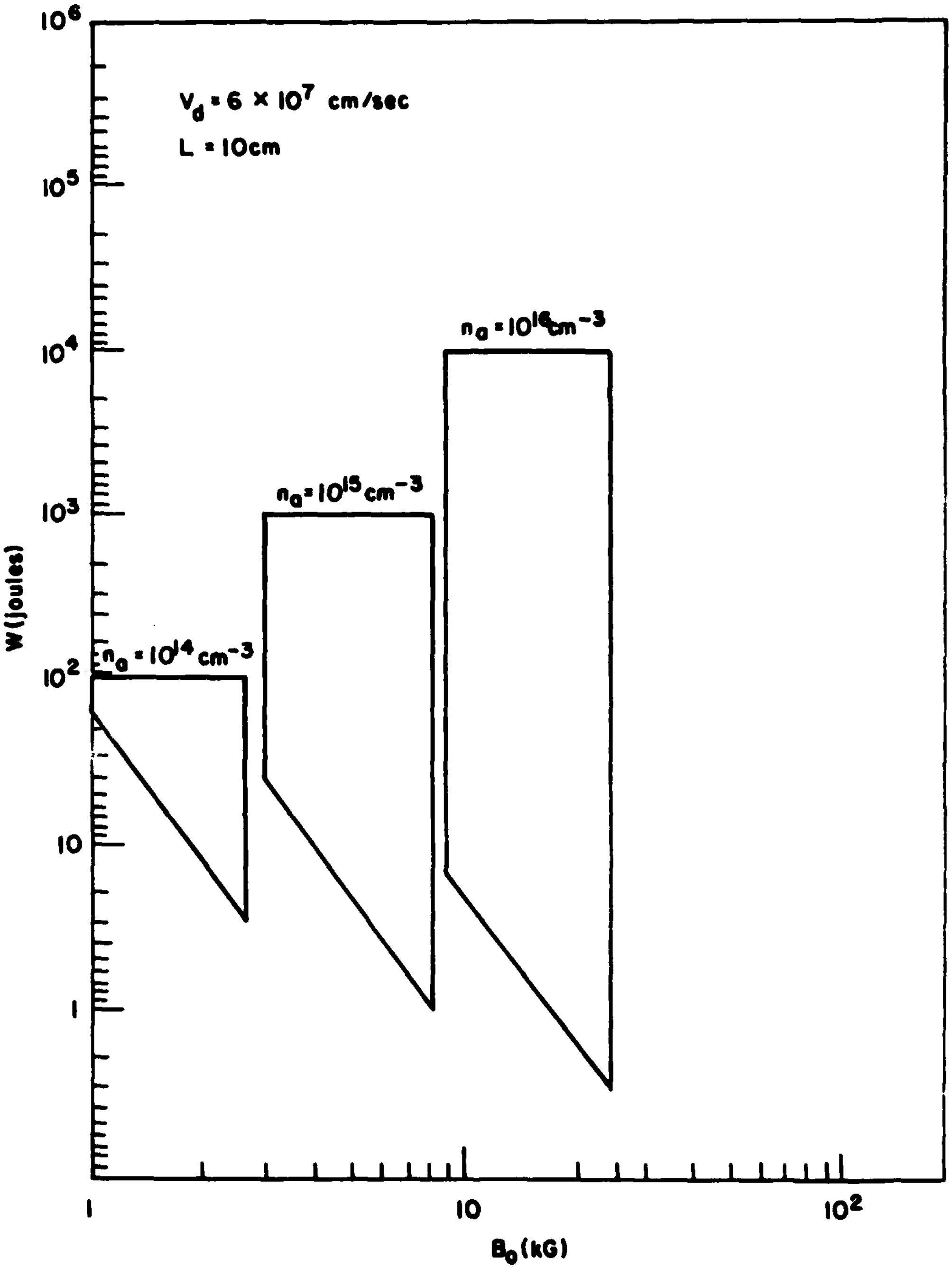

Figure 7

Plot of kinetic yield W (joules) versus ambient magnetic field B_0 (G) for the same target/gas as Fig. 6. We take $V_d = 6 \times 10^7$ cm/sec, L=10 cm, and $n_a = 10^{14}$, 10^{15}, and 10^{16} cm^{-3}.

ACKNOWLEDGMENTS

We thank Barry Ripin, Steve Kacenjar, and Jacob Grun for discussions of current experimental results and future plans, and Bob Clark and Dennis Papadopoulos for discussions regarding the coupling instabilities. We also thank Barry Ripin for a critical reading of the manuscript.

This research has been supported by the Defense Nuclear Agency.

REFERENCES

Cornwall, M. S. Flatté, D. Hammer, and J. Vesecky, "Studies of the effect of striations on radio communications," JASON report JSR-81-31, 1981.

Hyman, E., M. Mulbrandon, and J.D. Huba, "Preliminary report of UVDEP and PRODEP results for the NRL laser/HANE experiment," in preparation, 1983.

Lampe, M., W.L. Manheimer, and K. Papadopoulos, "Anomalous transport coefficients for HANE applications due to plasma microinstabilities," NRL Memo 3076, 1975.

Longmire, C., M. Alme, R. Kilb, and L. Wright, "Scaling of debris-air coupling," MRC Report AMRC-R-338, 1981.

McBride, J.B., E. Ott, J.B. Boris, and J.H. Orens, "Theory and simulation of turbulent heating by the modified two stream instability," Phys. Fluids, 15, 2367, 1972.

Papadopoulos, K., R.C. Davidson, J.M. Dawson, I. Haber, D.A. Hammer, N.A. Krall, and R. Shanny, "Heating of counterstreaming ion beams in an external magnetic field," Phys. Fluids, 14, 849, 1971.

Tsai, W., L.L. DeRaad, Jr., and R. LeLevier, "Scaling laws for simulating early-time high-altitude nuclear explosion phenomena," R & D Associates Report, 1982.

Vesecky, J.F., J.W. Chamberlain, J.M. Cornwall, D.A. Hammer, and F.W. Perkins, "Irregularities in ionospheric plasma clouds: Their evolution and effect on radio communication," JASON report JSR-80-15, 1980.

Wright, L., "Early-time model of laser plasma expansion," Phys. Fluids, 14, 1905, 1971.

DISTRIBUTION LIST

DEPARTMENT OF DEFENSE

ASSISTANT SECRETARY OF DEFENSE
COMM, CMD, CONT 7 INTELL
WASHINGTON, D.C. 20301

DIRECTOR
COMMAND CONTROL TECHNICAL CENTER
PENTAGON RM BE 685
WASHINGTON, D.C. 20301
01CY ATTN C-650
01CY ATTN C-312 R. MASON

DIRECTOR
DEFENSE ADVANCED RSCH PROJ AGENCY
ARCHITECT BUILDING
1400 WILSON BLVD.
ARLINGTON, VA. 22209
01CY ATTN NUCLEAR MONITORING RESEARCH
01CY ATTN STRATEGIC TECH OFFICE

DEFENSE COMMUNICATION ENGINEER CENTER
1860 WIEHLE AVENUE
RESTON, VA. 22090
01CY ATTN CODE R410
01CY ATTN CODE R812

DEFENSE TECHNICAL INFORMATION CENTER
CAMERON STATION
ALEXANDRIA, VA. 22314
02CY

DIRECTOR
DEFENSE NUCLEAR AGENCY
WASHINGTON, D.C. 20305
01CY ATTN STVL
04CY ATTN TITL
01CY ATTN DDST
03CY ATTN RAAE

COMMANDER
FIELD COMMAND
DEFENSE NUCLEAR AGENCY
KIRTLAND, AFB, NM 87115
01CY ATTN FCPR

DIRECTOR
INTERSERVICE NUCLEAR WEAPONS SCHOOL
KIRTLAND AFB, NM 87115
01CY ATTN DOCUMENT CONTROL

JOINT CHIEFS OF STAFF
WASHINGTON, D.C. 20301
01CY ATTN J-3 WWMCCS EVALUATION OFFICE

DIRECTOR
JOINT STRAT TGT PLANNING STAFF
OFFUTT AFB
OMAHA, NB 68113
01CY ATTN JLTW-2
01CY ATTN JPST G. GOETZ

CHIEF
LIVERMORE DIVISION FLD COMMAND DNA
DEPARTMENT OF DEFENSE
LAWRENCE LIVERMORE LABORATORY
P.O. BOX 808
LIVERMORE, CA 94550
01CY ATTN FCPRL

COMMANDANT
NATO SCHOOL (SHAPE)
APO NEW YORK 09172
01CY ATTN U.S. DOCUMENTS OFFICER

UNDER SECY OF DEF FOR RSCH & ENGRG
DEPARTMENT OF DEFENSE
WASHINGTON, D.C. 20301
01CY ATTN STRATEGIC & SPACE SYSTEMS (OS)

WWMCCS SYSTEM ENGINEERING ORG
WASHINGTON, D.C. 20305
01CY ATTN R. CRAWFORD

COMMANDER/DIRECTOR
ATMOSPHERIC SCIENCES LABORATORY
U.S. ARMY ELECTRONICS COMMAND
WHITE SANDS MISSILE RANGE, NM 88002
01CY ATTN DELAS-EO F. NILES

PRECEDING PAGE BLANK-NOT FILMED

DIRECTOR
BMD ADVANCED TECH CTR
HUNTSVILLE OFFICE
P.O. BOX 1500
HUNTSVILLE, AL 35807
  01CY ATTN ATC-T MELVIN T. CAPPS
  01CY ATTN ATC-O W. DAVIES
  01CY ATTN ATC-R DON RUSS

PROGRAM MANAGER
BMD PROGRAM OFFICE
5001 EISENHOWER AVENUE
ALEXANDRIA, VA 22333
  01CY ATTN DACS-BMT J. SHEA

CHIEF C-E- SERVICES DIVISION
U.S. ARMY COMMUNICATIONS CMD
PENTAGON RM 1B269
WASHINGTON, D.C. 20310
  01CY ATTN C- E-SERVICES DIVISION

COMMANDER
FRADCOM TECHNICAL SUPPORT ACTIVITY
DEPARTMENT OF THE ARMY
FORT MONMOUTH, N.J. 07703
  01CY ATTN DRSEL-NL-RD H. BENNET
  01CY ATTN DRSEL-PL-ENV H. BOMKE
  01CY ATTN J.E. QUIGLEY

COMMANDER
HARRY DIAMOND LABORATORIES
DEPARTMENT OF THE ARMY
2800 POWDER MILL ROAD
ADELPHI, MD 20783
  (CNWDI-INNER ENVELOPE: ATTN: DELHD-RBH)
  01CY ATTN DELHD-TI M. WEINER
  01CY ATTN DELHD-RB R. WILLIAMS
  01CY ATTN DELHD-NP C. MOAZED

COMMANDER
U.S. ARMY COMM-ELEC ENGRG INSTAL AGY
FT. HUACHUCA, AZ 85613
  01CY ATTN CCC-EMEO GEORGE LANE

COMMANDER
U.S. ARMY FOREIGN SCIENCE & TECH CTR
220 7TH STREET, NE
CHARLOTTESVILLE, VA 22901
  01CY ATTN DRXST-SD

COMMANDER
U.S. ARMY MATERIAL DEV & READINESS CMD
5001 EISENHOWER AVENUE
ALEXANDRIA, VA 22333
  01CY ATTN DRCLDC J.A. BENDER

COMMANDER
U.S. ARMY NUCLEAR AND CHEMICAL AGENCY
7500 BACKLICK ROAD
BLDG 2073
SPRINGFIELD, VA 22150
  01CY ATTN LIBRARY

DIRECTOR
U.S. ARMY BALLISTIC RESEARCH LABORATORY
ABERDEEN PROVING GROUND, MD 21005
  01CY ATTN TECH LIBRARY EDWARD BAICY

COMMANDER
U.S. ARMY SATCOM AGENCY
FT. MONMOUTH, NJ 07703
  01CY ATTN DOCUMENT CONTROL

COMMANDER
U.S. ARMY MISSILE INTELLIGENCE AGENCY
REDSTONE ARSENAL, AL 35809
  01CY ATTN JIM GAMBLE

DIRECTOR
U.S. ARMY TRADOC SYSTEMS ANALYSIS ACTIVITY
WHITE SANDS MISSILE RANGE, NM 88002
  01CY ATTN ATAA-SA
  01CY ATTN TCC/F. PAYAN JR.
  01CY ATTN ATTA-TAC LTC J. HESSE

COMMANDER
NAVAL ELECTRONIC SYSTEMS COMMAND
WASHINGTON, D.C. 20360
  01CY ATTN NAVALEX 034 T. HUGHES
  01CY ATTN PME 117
  01CY ATTN PME 117-T
  01CY ATTN CODE 5011

COMMANDING OFFICER
NAVAL INTELLIGENCE SUPPORT CTR
4301 SUITLAND ROAD, BLDG. 5
WASHINGTON, D.C. 20390
  01CY ATTN MR. DUBBIN STIC 12
  01CY ATTN NISC-50
  01CY ATTN CODE 5404 J. GALET

COMMANDER
NAVAL OCEAN SYSTEMS CENTER
SAN DIEGO, CA 92152
  01CY ATTN J. FERGUSON

DIRECTOR
NAVAL RESEARCH LABORATORY
WASHINGTON, D.C. 20375
  01CY ATTN CODE 4700 S. L. Ossakow
    26 CYS IF UNCLASS. 1 CY IF CLASS)
  01CY ATTN CODE 4701 I Vitkovitsky
  01CY ATTN CODE 4780 BRANCH HEAD (100
    CYS IF UNCLASS, 1 CY IF CLASS)
  01CY ATTN CODE 7500
  01CY ATTN CODE 7550
  01CY ATTN CODE 7580
  01CY ATTN CODE 7551
  01CY ATTN CODE 7555
  01CY ATTN CODE 4730 E. MCLEAN
  01CY ATTN CODE 4108
  01CY ATTN CODE 4730 B. RIPIN
  20CY ATTN CODE 2628

COMMANDER
NAVAL SEA SYSTEMS COMMAND
WASHINGTON, D.C. 20362
  01CY ATTN CAPT R. PITKIN

COMMANDER
NAVAL SPACE SURVEILLANCE SYSTEM
DAHLGREN, VA 22448
  01CY ATTN CAPT J.H. BURTON

OFFICER-IN-CHARGE
NAVAL SURFACE WEAPONS CENTER
WHITE OAK, SILVER SPRING, MD 20910
  01CY ATTN CODE F31

DIRECTOR
STRATEGIC SYSTEMS PROJECT OFFICE
DEPARTMENT OF THE NAVY
WASHINGTON, D.C. 20376
  01CY ATTN NSP-2141
  01CY ATTN NSSP-2722 FRED WIMBERLY

COMMANDER
NAVAL SURFACE WEAPONS CENTER
DAHLGREN LABORATORY
DAHLGREN, VA 22448
  01CY ATTN CODE DF-14 R. BUTLER

OFFICER OF NAVAL RESEARCH
ARLINGTON, VA 22217
  01CY ATTN CODE 465
  01CY ATTN CODE 461
  01CY ATTN CODE 402
  01CY ATTN CODE 420
  01CY ATTN CODE 421

COMMANDER
AEROSPACE DEFENSE COMMAND/DC
DEPARTMENT OF THE AIR FORCE
ENT AFB, CO 80912
  01CY ATTN DC MR. LONG

COMMANDER
AEROSPACE DEFENSE COMMAND/XPD
DEPARTMENT OF THE AIR FORCE
ENT AFB, CO 80912
  01CY ATTN XPDQQ
  01CY ATTN XP

AIR FORCE GEOPHYSICS LABORATORY
HANSCOM AFB, MA 01731
  01CY ATTN OPR HAROLD GARDNER
  01CY ATTN LKB KENNETH S.W. CHAMPION
  01CY ATTN OPR ALVA T. STAIR
  01CY ATTN PHD JURGEN BUCHAU
  01CY ATTN PHD JOHN P. MULLEN

AF WEAPONS LABORATORY
KIRTLAND AFT, NM 87117
  01CY ATTN SUL
  01CY ATTN CA ARTHUR H. GUENTHER
  01CY ATTN NTYCE 1LT. G. KRAJEI

AFTAC
PATRICK AFB, FL 32925
  01CY ATTN TF/MAJ WILEY
  01CY ATTN TN

AIR FORCE AVIONICS LABORATORY
WRIGHT-PATTERSON AFB, OH 45433
  01CY ATTN AAD WADE HUNT
  01CY ATTN AAD ALLEN JOHNSON

DEPUTY CHIEF OF STAFF
RESEARCH, DEVELOPMENT, & ACQ
DEPARTMENT OF THE AIR FORCE
WASHINGTON, D.C. 20330
  01CY ATTN AFRDQ

HEADQUATERS
ELECTRONIC SYSTEMS DIVISION/XR
DEPARTMENT OF THE AIR FORCE
HANSCOM AFB, MA 01731
  01CY ATTN XR J. DEAS

HEADQUATERS
ELECTRONIC SYSTEMS DIVISION/YSEA
DEPARTMENT OF THE AIR FORCE
HANSCOM AFB, MA 01732
  01CY ATTN YSEA

HEADQUATERS
ELECTRONIC SYSTEMS DIVISION/DC
DEPARTMENT OF THE AIR FORCE
HANSCOM AFB, MA 01731
  01CY ATTN DCKC MAJ J.C. CLARK

COMMANDER
FOREIGN TECHNOLOGY DIVISION, AFSC
WRIGHT-PATTERSON AFB, OH 45433
  01CY ATTN NICD LIBRARY
  01CY ATTN ETDP B. BALLARD

COMMANDER
ROME AIR DEVELOPMENT CENTER, AFSC
GRIFFISS AFB, NY 13441
  01CY ATTN DOC LIBRARY/TSLD
  01CY ATTN OCSE V. COYNE

SAMSO/SZ
POST OFFICE BOX 92960
WORLDWAY POSTAL CENTER
LOS ANGELES, CA 90009
  (SPACE DEFENSE SYSTEMS)
  01CY ATTN SZJ

STRATEGIC AIR COMMAND/XPFS
OFFUTT AFB, NB 68113
  01CY ATTN ADWATE MAJ BRUCE BAUER
  01CY ATTN NRT
  01CY ATTN DOK CHIEF SCIENTIST

SAMSO/SK
P.O. BOX 92960
WORLDWAY POSTAL CENTER
LOS ANGELES, CA 90009
  01CY ATTN SKA (SPACE COMM SYSTEMS)
    M. CLAVIN

SAMSO/MN
NORTON AFB, CA 92409
(MINUTEMAN)
  01CY ATTN MNNL

COMMANDER
ROME AIR DEVELOPMENT CENTER, AFSC
HANSCOM AFB, MA 01731
  01CY ATTN EEP A. LORENTZEN

DEPARTMENT OF ENERGY
LIBRARY ROOM G-042
WASHINGTON, D.C. 20545
  01CY ATTN DOC CON FOR A. LABOWITZ

DEPARTMENT OF ENERGY
ALBUQUERQUE OPERATIONS OFFICE
P.O. BOX 5400
ALBUQUERQUE, NM 87115
  01CY ATTN DOC CON FOR D. SHERWOOD

EG&G, INC.
LOS ALAMOS DIVISION
P.O. BOX 809
LOS ALAMOS, NM 85544
  01CY ATTN DOC CON FOR J. BREEDLOVE

UNIVERSITY OF CALIFORNIA
LAWRENCE LIVERMORE LABORATORY
P.O. BOX 808
LIVERMORE, CA 94550
  01CY ATTN DOC CON FOR TECH INFO DEPT
  01CY ATTN DOC CON FOR L-389 R. OTT
  01CY ATTN DOC CON FOR L-31 R. HAGER
  01CY ATTN DOC CON FOR L-46 F. SEWARD

LOS ALAMOS NATIONAL LABORATORY
P.O. BOX 1663
LOS ALAMOS, NM 87545
  01CY ATTN DOC CON FOR J. WOLCOTT
  01CY ATTN DOC CON FOR R.F. TASCHEK
  01CY ATTN DOC CON FOR E. JONES
  01CY ATTN DOC CON FOR J. MALIK
  01CY ATTN DOC CON FOR R. JEFFRIES
  01CY ATTN DOC CON FOR J. ZINN
  01CY ATTN DOC CON FOR P. KEATON
  01CY ATTN DOC CON FOR D. WESTERVELT

SANDIA LABORATORIES
P.O. BOX 5800
ALBUQUERQUE, NM 87115
  01CY ATTN DOC CON FOR W. BROWN
  01CY ATTN DOC CON FOR A. THORNBROUGH
  01CY ATTN DOC CON FOR T. WRIGHT
  01CY ATTN DOC CON FOR D. DAHLGREN
  01CY ATTN DOC CON FOR 3141
  01CY ATTN DOC CON FOR SPACE PROJECT DIV

SANDIA LABORATORIES
LIVERMORE LABORATORY
P.O. BOX 969
LIVERMORE, CA 94550
  01CY ATTN DOC CON FOR B. MURPHEY
  01CY ATTN DOC CON FOR T. COOK

OFFICE OF MILITARY APPLICATION
DEPARTMENT OF ENERGY
WASHINGTON, D.C. 20545
  01CY ATTN DOC CON DR. YO SONG

OTHER GOVERNMENT

DEPARTMENT OF COMMERCE
NATIONAL BUREAU OF STANDARDS
WASHINGTON, D.C. 20234
(ALL CORRES: ATTN SEC OFFICER FOR)
01CY ATTN R. MOORE

INSTITUTE FOR TELECOM SCIENCES
NATIONAL TELECOMMUNICATIONS & INFO ADMIN
BOULDER, CO 80303
01CY ATTN A. JEAN (UNCLASS ONLY)
01CY ATTN W. UTLAUT
01CY ATTN D. CROMBIE
01CY ATTN L. BERRY

NATIONAL OCEANIC & ATMOSPHERIC ADMIN
ENVIRONMENTAL RESEARCH LABORATORIES
DEPARTMENT OF COMMERCE
BOULDER, CO 80302
01CY ATTN R. GRUBB
01CY ATTN AERONOMY LAB G. REID

DEPARTMENT OF DEFENSE CONTRACTORS

AEROSPACE CORPORATION
P.O. BOX 92957
LOS ANGELES, CA 90009
01CY ATTN I. GARFUNKEL
01CY ATTN T. SALMI
01CY ATTN V. JOSEPHSON
01CY ATTN S. BOWER
01CY ATTN D. OLSEN

ANALYTICAL SYSTEMS ENGINEERING CORP
5 OLD CONCORD ROAD
BURLINGTON, MA 01803
01CY ATTN RADIO SCIENCES

BERKELEY RESEARCH ASSOCIATES, INC.
P.O. BOX 983
BERKELEY, CA 94701
01CY ATTN J. WORKMAN
01CY ATTN C. PRETTIE
01CY ATTN S. BRECHT

BOEING COMPANY, THE
P.O. BOX 3707
SEATTLE, WA 98124
01CY ATTN G. KEISTER
01CY ATTN D. MURRAY
01CY ATTN G. HALL
01CY ATTN J. KENNEY

CALIFORNIA AT SAN DIEGO, UNIV OF
P.O. BOX 6049
SAN DIEGO, CA 92106

CHARLES STARK DRAPER LABORATORY, INC.
555 TECHNOLOGY SQUARE
CAMBRIDGE, MA 02139
01CY ATTN D.B. COX
01CY ATTN J.P. GILMORE

COMSAT LABORATORIES
LINTHICUM ROAD
CLARKSBURG, MD 20734
01CY ATTN G. HYDE

CORNELL UNIVERSITY
DEPARTMENT OF ELECTRICAL ENGINEERING
ITHACA, NY 14850
01CY ATTN D.T. FARLEY, JR.

ELECTROSPACE SYSTEMS, INC.
BOX 1359
RICHARDSON, TX 75080
01CY ATTN H. LOGSTON
01CY ATTN SECURITY (PAUL PHILLIPS)

EOS TECHNOLOGIES, INC.
606 Wilshire Blvd.
Santa Monica, Calif 90401
01CY ATTN C.B. GABBARD

ESL, INC.
495 JAVA DRIVE
SUNNYVALE, CA 94086
01CY ATTN J. ROBERTS
01CY ATTN JAMES MARSHALL

GENERAL ELECTRIC COMPANY
SPACE DIVISION
VALLEY FORGE SPACE CENTER
GODDARD BLVD KING OF PRUSSIA
P.O. BOX 8555
PHILADELPHIA, PA 19101
01CY ATTN M.H. BORTNER SPACE SCI LAB

GENERAL ELECTRIC COMPANY
P.O. BOX 1122
SYRACUSE, NY 13201
01CY ATTN F. REIBERT

GENERAL ELECTRIC TECH SERVICES CO., INC.
HMES
COURT STREET
SYRACUSE, NY 13201
01CY ATTN G. MILLMAN

GEOPHYSICAL INSTITUTE
UNIVERSITY OF ALASKA
FAIRBANKS, AK 99701
(ALL CLASS ATTN: SECURITY OFFICER)
01CY ATTN T.N. DAVIS (UNCLASS ONLY)
01CY ATTN TECHNICAL LIBRARY
01CY ATTN NEAL BROWN (UNCLASS ONLY)

GTE SYLVANIA, INC.
ELECTRONICS SYSTEMS GRP-EASTERN DIV
77 A STREET
NEEDHAM, MA 02194
01CY ATTN DICK STEINHOF

HSS, INC.
2 ALFRED CIRCLE
BEDFORD, MA 01730
01CY ATTN DONALD HANSEN

ILLINOIS, UNIVERSITY OF
107 COBLE HALL
150 DAVENPORT HOUSE
CHAMPAIGN, IL 61820
(ALL CORRES ATTN DAN MCCLELLAND)
01CY ATTN K. YEH

INSTITUTE FOR DEFENSE ANALYSES
1801 NO. BEARUEGARD STREET
ALEXANDRIA, VA 22202
01CY ATTN J.M. AEIN
01CY ATTN ERNEST BAUER
01CY ATTN HANS WOLFARD
01CY ATTN JOEL BENGSTON

INTL TEL & TELEGRAPH CORPORATION
500 WASHINGTON AVENUE
NUTLEY, NJ 07110
01CY ATTN TECHNICAL LIBRARY

JAYCOR
11011 TORREYANA ROAD
P.O. BOX 85154
SAN DIEGO, CA 92138
01CY ATTN J.L. SPERLING

JOHNS HOPKINS UNIVERSITY
APPLIED PHYSICS LABORATORY
JOHNS HOPKINS ROAD
LAURAL, MD 20810
01CY ATTN DOCUMENT LIBRARIAN
01CY ATTN THOMAS POTEMRA
01CY ATTN JOHN DASSOULAS

KAMAN SCIENCES CORP
P.O. BOX 7463
COLORADO SPRINGS, CO 80933
01CY ATTN T. MEAGHER

KAMAN TEMPO-CENTER FOR ADVANCED STUDIES
816 STATE STREET (P.O DRAWER QQ)
SANTA BARBARA, CA 93102
01CY ATTN DASIAC
01CY ATTN WARREN S. KNAPP
01CY ATTN WILLIAM MCNAMARA
01CY ATTN B. GAMBILL

LINKABIT CORP
10453 ROSELLE
SAN DIEGO, CA 92121
01CY ATTN IRWIN JACOBS

LOCKHEED MISSILES & SPACE CO., INC
P.O. BOX 504
SUNNYVALE, CA 94088
01CY ATTN DEPT 60-12
01CY ATTN D.R. CHURCHILL

LOCKHEED MISSILES & SPACE CO., INC.
3251 HANOVER STREET
PALO ALTO, CA 94304
01CY ATTN MARTIN WALT DEPT 52-12
01CY ATTN W.L. IMHOF DEPT 52-12
01CY ATTN RICHARD G. JOHNSON DEPT 52-12
01CY ATTN J.B. CLADIS DEPT 52-12

MARTIN MARIETTA CORP
ORLANDO DIVISION
P.O. BOX 5837
ORLANDO, FL 32805
01CY ATTN R. HEFFNER

M.I.T. LINCOLN LABORATORY
P.O. BOX 73
LEXINGTON, MA 02173
01CY ATTN DAVID M. TOWLE
01CY ATTN L. LOUGHLIN
01CY ATTN D. CLARK

MCDONNEL DOUGLAS CORPORATION
5301 BOLSA AVENUE
HUNTINGTON BEACH, CA 92647
01CY ATTN N. HARRIS
01CY ATTN J. MOULE
01CY ATTN GEORGE MROZ
01CY ATTN W. OLSON
01CY ATTN R.W. HALPRIN
01CY ATTN TECHNICAL LIBRARY SERVICES

MISSION RESEARCH CORPORATION
735 STATE STREET
SANTA BARBARA, CA 93101
  01CY ATTN P. FISCHER
  01CY ATTN W.F. CREVIER
  01CY ATTN STEVEN L. GUTSCHE
  01CY ATTN D. SAPPENFIELD
  01CY ATTN R. BOGUSCH
  01CY ATTN R. HENDRICK
  01CY ATTN RALPH KILB
  01CY ATTN DAVE SOWLE
  01CY ATTN F. FAJEN
  01CY ATTN M. SCHEIBE
  01CY ATTN CONRAD L. LONGMIRE

MITRE CORPORATION, THE
P.O. BOX 208
BEDFORD, MA 01730
  01CY ATTN JOHN MORGANSTERN
  01CY ATTN G. HARDING
  01CY ATTN C.E. CALLAHAN

MITRE CORP
WESTGATE RESEARCH PARK
1820 DOLLY MADISON BLVD
MCLEAN, VA 22101
  01CY ATTN W. HALL
  01CY ATTN W. FOSTER

PACIFIC-SIERRA RESEARCH CORP
12340 SANTA MONICA BLVD.
LOS ANGELES, CA 90025
  01CY ATTN E.C. FIELD, JR.

PENNSYLVANIA STATE UNIVERSITY
IONOSPHERE RESEARCH LAB
318 ELECTRICAL ENGINEERING EAST
UNIVERSITY PARK, PA 16802
  (NO CLASS TO THIS ADDRESS)
  01CY ATTN IONOSPHERIC RESEARCH LAB

PHOTOMETRICS, INC.
4 ARROW DRIVE
WOBURN, MA 01801
  01CY ATTN IRVING L. KOFSKY

PHYSICAL DYNAMICS, INC.
P.O. BOX 3027
BELLEVUE, WA 98009
  01CY ATTN E.J. FREMOUW

PHYSICAL DYNAMICS, INC.
P.O. BOX 10367
OAKLAND, CA 94610
  ATTN A. THOMSON

R & D ASSOCIATES
P.O. BOX 9695
MARINA DEL REY, CA 90291
  01CY ATTN FORREST GILMORE
  01CY ATTN WILLIAM B. WRIGHT, JR.
  01CY ATTN ROBERT F. LELEVIER
  01CY ATTN WILLIAM J. KARZAS
  01CY ATTN H. ORY
  01CY ATTN C. MACDONALD
  01CY ATTN R. TURCO

RAND CORPORATION, THE
1700 MAIN STREET
SANTA MONICA, CA 90406
  01CY ATTN CULLEN CRAIN
  01CY ATTN ED BEDROZIAN

RAYTHEON CO.
528 BOSTON POST ROAD
SUDBURY, MA 01776
  01CY ATTN BARBARA ADAMS

RIVERSIDE RESEARCH INSTITUTE
80 WEST END AVENUE
NEW YORK, NY 10023
  01CY ATTN VINCE TRAPANI

SCIENCE APPLICATIONS, INC.
P.O. BOX 2351
LA JOLLA, CA 92038
  01CY ATTN LEWIS M. LINSON
  01CY ATTN DANIEL A. HAMLIN
  01CY ATTN E. FRIEMAN
  01CY ATTN E.A. STRAKER
  01CY ATTN CURTIS A. SMITH
  01CY ATTN JACK MCDOUGALL

SCIENCE APPLICATIONS, INC
1710 GOODRIDGE DR.
MCLEAN, VA 22102
  ATTN: J. COCKAYNE

SRI INTERNATIONAL
333 RAVENSWOOD AVENUE
MENLO PARK, CA 94025
01CY ATTN DONALD NEILSON
01CY ATTN ALAN BURNS
01CY ATTN G. SMITH
01CY ATTN R. TSUNODA
01CY ATTN DAVID A. JOHNSON
01CY ATTN WALTER G. CHESNUT
01CY ATTN CHARLES L. RINO
01CY ATTN WALTER JAYE
01CY ATTN J. VICKREY
01CY ATTN RAY L. LEADABRAND
01CY ATTN G. CARPENTER
01CY ATTN G. PRICE
01CY ATTN J. PETERSON
01CY ATTN R. LIVINGSTON
01CY ATTN V. GONZALES
01CY ATTN D. MCDANIEL

STEWART RADIANCE LABORATORY
UTAH STATE UNIVERSITY
1 DE ANGELO DRIVE
BEDFORD, MA 01730
01CY ATTN J. ULWICK

TECHNOLOGY INTERNATIONAL CORP
75 WIGGINS AVENUE
BEDFORD, MA 01730
01CY ATTN W.P. BOQUIST

TOYON
34 WALNUT LAND
SANTA BARBARA, CA 93111
01CY ATTN JOHN ISE, JR.
01CY ATTN JOEL GARBARINO

TRW DEFENSE & SPACE SYS GROUP
ONE SPACE PARK
REDONDO BEACH, CA 90278
01CY ATTN R. K. PLEBUCH
01CY ATTN S. ALTSCHULER
01CY ATTN D. DEE
P1CY ATTM D/ Stockwell
SNTF/1575

VISIDYNE
SOUTH BEDFORD STREET
BURLINGTON, MASS 01803
01CY ATTN W. REIDY
01CY ATTN J. CARPENTER
01CY ATTN C. HUMPHREY